Effect of Solvent on the Self-Assembly of Dialanine and Diphenylalanine Peptides

A. Rissanou and E. Georgilis and E. Kasotakis and A. Mitraki and Vagelis A. Harmandaris

Effect of Solvent on the Self-Assembly of Dialanine and Diphenylalanine Peptides

Anastassia N. Rissanou[1,2,*], Evangelos Georgilis[3], Emmanouil Kasotakis[3], Anna Mitraki[3,4] and Vagelis Harmandaris[1,2,*]

1. Department of Applied Mathematics, University of Crete, GR-71409, Heraklion, Crete, Greece
2. IACM FORTH, GR-71110 Heraklion, Crete, Greece.
3. Department of Materials Science and Technology, University of Crete, Greece.
4. Institute for Electronic Structure and Laser, FORTH, Heraklion, Crete, Greece

[*] Authors to whom correspondence should be addressed:
rissanou@tem.uoc.gr +30 2810393746 fax: +30 2810393701
vagelis@tem.uoc.gr +30 2810393735 fax: +30 2810393701

Keywords: Peptides, Self-assembly, Water, Methanol, Molecular Dynamics

Abstract

Diphenylalanine (FF) is a very common peptide with many potential applications, both biological and technological, due to a large number of different nanostructures which it attains. The current work concerns a detailed study of the self assembled structures of FF in two different solvents, an aqueous (H_2O) and an organic (CH_3OH) through simulations and experiments. Detailed atomistic Molecular Dynamics (MD) simulations of FF in both solvents have been performed, using an explicit solvent model. The self assembling propensity of FF in water is obvious while in methanol a very weak self assembling propensity is observed. We studied and compared structural properties of FF in the two different solvents and a comparison with a system of dialanine (AA) in the corresponding solvents was also performed. In addition, temperature dependence studies were carried out. Finally, the simulation predictions were compared to new experimental data, which were produced in the framework of the present work. A very good qualitative agreement between simulation and experimental observations was found.

I. Introduction

Numerous supramolecular protein assemblies have been demonstrated to have either physiological or pathological activities. The most significant case of disease-associated self-organized structures is that of amyloid fibrils, whose formation is the hallmark of major human disorders. Amino acid composition plays a fundamental role on the conformations and stability of proteins in solution. For this reason the observation of their physical and chemical properties constitutes the focus of many experimental and computational studies[1,2,3,4,5].

A very common, but of particular interest peptide, is diphenylalanine (**peptide, FF)** which is the core recognition motif of Alzheimer's β-amyloid peptide. One especially intriguing feature which was observed by experimental observations[6,7,8,9] on diphenylalanine peptide is that the same building block can self-assemble either into fibrillar, or spherical structures depending on conditions such as solvent and temperature[10,11]. The aromatic phenylalanine rings seem to play a critical role in the self-assembly, probably through π-π* stacking interactions, as first postulated by Gazit[12]. The first experimental support for this critical role came through a systematic alanine scan in the core recognition motif of the islet amyloid, NFGAIL. Replacement of Asn 1 and Gly 3 by Ala did not inhibit amyloid fibril formation, whereas replacement of Phe 3 abolished the aggregate formation ability[13].

Huang et al.[14] have examined the effect of binary solvent systems on the ability of FF to form either nanofibers or nanotubes after heating at $95^{o}C$ and subsequent cooling in solution, or alternatively, deposition on surfaces. Interestingly, they have reported that upon cooling from mixed water- methanol systems, nanofibers can form in solution, but

no formation is observed when the percentage of methanol exceeds *70%*. In these conditions, nanofibers form only upon drying on glass surfaces. The authors attributed this behavior to the ability of methanol to form hydrogen bonds with the diphenylalanine molecules, leading to good solvation of peptide molecules, making therefore difficult their migration from their solvation shell towards formation of assemblies.

Moreover, experimental observations indicate that the properties of FF peptide can be modulated by N-termini blocking, amino acid changes, or conjugation to other chemical moieties[6,15,16,17,18].

In addition, there are various experiments which demonstrate the effect of alcohol on the structure of proteins, when it is added in aqueous solutions[19,20]. Methanol is a widely used solvent in the protein folding and structure investigations[20]. Hwang et al.[21], in a combined theoretical and experimental study, showed that the addition of methanol in an aqueous solution of a model peptide BBA5 enhances the formation of secondary structure. Methanol is responsible for the weakening of the hydrophobic interactions and at the same time the strengthening of the backbone-backbone interactions of the peptide.

The theoretical principles that govern self-assembly and polymorphism of these building blocks are currently unknown, and will provide precious insight towards understanding and rational design of new generations of self-assembled nanostructures. Besides experiments, computer simulations could contribute to the clarification of some of the basic questions related to the structural and dynamical properties of FF peptide under various conditions.

Interesting computer simulations studies of diphenylalanine peptide in aqueous solutions have been performed both in all atom and coarse-grained models[22,23,24,25].

Tamamis et al.[22] explored the self-assembly of FF and FFF peptides in aqueous solution, using the replica exchange method in an implicit solvent model. They observed open and ring-like peptide networks, especially for FFF, consistent with the nanostructures observed in experiments. Villa et al.[23], developed a coarse grained model for FF in aqueous solution, and studied the self-assembly and conformational properties of FF in both explicit and implicit solvent representation. Another interesting molecular dynamics study[26] presents the solvation properties of four non-polar amino acids: alanine, valine, leucine and phenylalanine, in water and in methanol at infinite dilution (i.e., isolated molecule in solvent). Their simulations revealed that the solvation structures are richer for methanol than for water. Frederix et al.[24] presented the aggregation propensity of all 400 dipeptides of the 20 gene-encoded amino acids, through a Molecular dynamics study, based on a coarse grained force field**.** One of these dipeptides was diphenylalanine, where the supramolecular structures in aqueous solution, predicted by the coarse grained model, are in good agreement with corresponding experimental results. Using a similar coarse grained model, Guo et al.[25] presented interesting results for the nanostructures of diphenylalanine peptides in aqueous solution. A variety of ordered nanostructures was detected while the assembly pathways were found to be concentration dependent. Moreover, they underlined that the aromatic stacking interaction provides the driving force for the self assembly procedure.

The current study is the first stage of a general computational approach for the study of self-assembling peptides. Our goal is to predict, from first principles, the various structures formed from different peptides and also to examine the effect of different solvents. Here we present a detailed comparison of the behavior of dialanine and

diphenylalanine peptide in two different solvents, water and methanol, in terms of structural properties through atomistic Molecular Dynamic simulations, using an explicit solvent model. The effect of temperature on the properties of the system, in both solvents, is studied as well. Experimental observations will be used for qualitative comparisons with the model results.

The paper is organized as follows. Section II provides detailed information about (a) the experimental procedure , and (b) the simulation methodology as well as the model systems studied in this work. Our simulation results are presented in Section III, where a division in different subsections according to the different studied properties has been made. The experimental observations are depicted in Section IV. Finally, Section V contains a discussion and the conclusions of the current study.

II. Systems and Methods

a) Experimental Details

The FF peptide with free N- and C-termini was purchased from Bachem in the form of lyophilized powder with purity > *95%*. The powder was dissolved in water (*pH: 7.14*) or in methanol at concentrations of *2mg/mL* ($2 \cdot 10^{-3} gr/cm^3$). The dissolution of the peptide powders was achieved with addition of the peptide and solvent in a glass vial, then subsequent heating at 55^oC in a water bath for thirty minutes, using sonication for *20s* every five minutes of heating. Subsequently, half of the sample volume remained incubated in 55^oC, while the other half was transferred in a glass vial pre-incubated in

27°C. This particular protocol involves dissolving the peptide powder in high temperature followed by subsequent transfer to ambient temperatures in order to induce FF self-assembly and was first described by Song et al.[10]. It was adopted here in order to avoid the use of cosolvents such as hexafluoroisopropanol (HFIP) for dissolving the peptide powders which is followed by dilution into water (or the desired solvent) for induction of self-assembly. The above procedure ensures a similar protocol for the systems studied through both molecular simulations and experiments. The samples were observed for the formation of visible precipitates in solution. Sample solutions of *10μL* from both vials were deposited on glass slides instantly after separating the samples, then after *30min*, *1h* and *2h* of incubation. The sample solutions were dried in air, covered with *15nm* of gold sputtering and observed by Scanning Electron Microscopy (S.E.M.). S.E.M. experiments were performed at the Department of Biology of the University of Crete by using a JEOL JSM-6390LV microscope operating at *15kV*.

b) Simulation Methodology

The systems studied in this work are depicted in Table 1. Setup details, such as the number of the peptides, the number of solvent molecules, the total number of atoms in the simulation and the temperature in *K* are included in Table 1. The concentration is equal to $c=0.0385 grFF/cm^3 solvent$ for all systems. The behavior of di-alanine (AA) and di-phenylalanine (FF) was examined in two solvents, an aqueous and an organic, methanol, at a range of temperatures of about *50K* and at two different concentrations. A direct comparison between the two peptides illustrates the effect of phenyl groups on various properties.

The atomistic structures of FF in water and in methanol are presented in Figure 1a and 1b respectively. Note the slight difference in terminal groups of FF in the two solvents, in consistency with experimental sequences. Atomistic Molecular Dynamics (MD) simulations in the *NPT* statistical ensemble were performed using GROMACS code[27,28,29]. The pressure was kept constant at *P=1atm*, using a Berendsen barostat, while the stochastic velocity rescaling thermostat[30] was used to maintain the temperature value. All parameters for the description of intermolecular and intramolecular interactions were taken from the GROMOS53a6[31] force field. For the aqueous solutions the SPC model[32] for water was used. An all atom representation was applied except from CH methyl group of molecule's backbone and CH_2 which connects the backbone with the phenyl group, which have been applied as united atoms. The time step was *0.001ps* and a cutoff of *10Å* for both electrostatic and non bonded interaction was used. Bond lengths were constrained by means of 'LINCS' algorithm. All systems were equilibrated for *100ns* and production runs of another *100ns* were performed. The equilibration of the systems has been checked through two typical tests. The observation of the time evolution of the potential energy at different windows of time of the production run, as well as, the calculation of the radial distribution function, from data which correspond to different windows of time of the production run. Both quantities sue for equilibrated systems.

Simulations for di-phenylalanine in both solvents were also performed using the replica-exchange method[33,34,35,36,37,38]. We employed 16 replicas with temperatures in the range of [*295-343*]K for FF in water and [*285-332*]K for FF in methanol, with a step determined by the exponential relation: $T(i) = T_{init} e^{k*i}$, where T_{init} is the initial temperature, *i* is the number of replicas and *k* is a multiplying constant (*k=0.01*). Replica

exchanges were attempted at *1p*s intervals in water and at *0.2ps* in methanol and the total simulation length at each temperature was *150ns* for solutions in water, and *70ns* for solutions in methanol. The average number of exchanges between adjacent replicas was around *6%* for FF in water and *17%* for FF in methanol. These simulations were also used as part of the equilibration procedure. Note also that the acceptance ratio for replica exchanges for FF in water is relatively small. Additional shorter replica runs, with a larger number of replicas and smaller temperature step of about *2* degrees, have given an acceptance ratio of *24%* and identical results.

III. Simulation Results

a) Potential of Mean Force Between 2 Peptides

We start the discussion of simulation results by studying the interaction between two isolated peptides dissolved in water or in methanol. This interaction can be quantified by calculating the potential of mean force (PMF) which describes the effective interaction between two molecules in a medium. In order to calculate PMF we keep the distance between the centers of mass (cm) of two molecules constant and perform long simulations that allow the full sampling of phase space in this configuration. Finally we repeat these simulations for a series of different cm-cm distances. PMF is obtained by integrating the mean force from an ensemble of configurations and is corrected by adding an entropy term because of the cm-cm distance constraint (i.e due to the rotation of the cms), through:

$$U(r) = \int_{r_{\max}}^{r} F(r)dr - 2k_B T \ln r \,. \qquad (1)$$

In the above equation $U(r)$ is the PMF as a function of distance (r), r_{max} is the maximum distance between the two molecules, beyond which $U(r)$ equals to zero, $F(r)$ is the mean force and T is the temperature.

The potentials of mean force for Dialanine (AA) and Diphenylalanine (FF) in water and in methanol as a function of distance between the centers of mass of the two corresponding molecules are presented in Figure 2a and 2b respectively. With solid horizontal lines thermal energy (k_BT) is also shown. Starting with water and comparing the PMF of FF and AA we observe that for both molecules it is repulsive at short distances, it presents an attractive well for cm-cm distances between *0.5nm* and *1.7nm* for FF and between *0.6nm* and *1.6nm* for AA and it becomes zero at longer distances. The main difference is the depth of this attractive well which is equal to $7.1k_BT$ for FF, while for AA it is much lower, equal to $2.9k_BT$. This observation indicates that the phenyl groups of FF are responsible for the stronger attraction between the molecules. On the other hand, the PMF in methanol is totally repulsive for both AA and FF. Another observation is that PMF curves for AA and FF in water are slightly steeper than the ones in methanol.

In the next sections (***b, c***) we analyze the bulk properties of peptides at room temperature, *T=300K* and at concentration $c=0.0385 grFF/cm^3 solvent$. The temperature dependence of the self-assembly will be presented in a separate section.

b) Structural Properties

The mean size of an FF molecule in water and in methanol is quantified by the radius of gyration of the peptide which is given by the following equation: $< R_g >= \sqrt{\left\langle \frac{\sum_i m_i (r_i - R_{cm})^2}{\sum_i m_i} \right\rangle}$ and is equal to (*0.361±0.06*)nm in water and (*0.395±0.08*)nm in methanol. FF is slightly larger in methanol compared to its size in water, which means that methanol can be thought as a rather better solvent for FF. Interestingly, di-alanine (AA) has the same dimensions in water and in methanol with an $<R_g>$ = (*0.254±0.001*)nm, which brings out the hydrophobicicity of phenyl groups.

Structure of peptides, in the level of molecule center-of-mass, can be studied by calculating the pair radial distribution functions (rdf). Data about the rdf of peptides in the two solvents are presented in Figure 3. Figure 3a depicts the rdf between FF molecules and between AA molecules in water and Figure 3b in methanol, calculated for the centers of mass of the molecules. A comparison of the rdf curves for FF in the two solvents makes clear that there is a strong tendency for self assembly of FF in water in contrast to its behavior in methanol. The large peak of rdf in water in addition to the tail of the curve, which tends to zero for large distances, indicates the high probability of FF molecules to be close to one another and to exclude water molecules from their region.

For FF in methanol, rdf has a substantial smaller peak at short distances and a tail which tends to one for long distances. These features show an almost homogeneous distribution of FF molecules in methanol; consequently there is no evidence for self assembly through rdf's of center-of-mass. A comparison between rdf curves of FF and AA in water reveals a huge difference in the value of the first peak in addition to the tail's values which tend to one for AA and to zero for FF. This observation suggests that the

phenyl groups are the cause of the strong self-assembly. However, rdf for AA in water indicates the existence of some structure in AA aqueous solutions as well. On the contrary rdf curves of FF and AA in methanol do not appear substantial structure.

The pair radial distribution functions between FF molecules and solvent molecules are presented in Figure 3c. This figure provides supplemental information for the arrangement of FF peptides in water and in methanol, which is consistent to the above discussion. FF molecules exclude water from their vicinity because they prefer to form self assembled structures and as a result the values of rdf, at short distances, are much lower than one, whereas at higher distances they tend to unity. On the other hand the FF-methanol rdf curve is almost structureless, indicating an equal probability for methanol molecules to be everywhere in the solution.

Figure 4 contains pictures of the two model systems which are illustrative of the previous description. Figure 4a is a snapshot of FF in water and Figure 4b is a snapshot of FF in methanol. In both snapshots the number of FF molecules in the system is the same, 16, while a different number of solvent molecules are included according to the description of Table 1 (systems 3 and 4). For reasons of distinctness solvent molecules are presented as ghost molecules. Self assembly is obvious in water whereas the structure in methanol is substantially less ordered.

Another interesting issue is the way that FF molecules are positioned in both solvents, in terms of the preferable orientation of one peptide with regard to the orientation of another peptide which has a constant cm-cm distance from the first. For this reason a number of simulation runs for a pair of FF peptides were performed, for a series of different cm-cm constant distances. The preferable orientation of FF molecules

is quantified by the dot product of the end to end vectors of the two molecules. The probability distribution of θ – value, $P(\theta)$, at different cm–cm distances, is presented in Figure 5a for FF in water and Figure 5b for FF in methanol. The main feature of Figures 5a and 5b is that the peptides prefer to orient antiparallel at short distances in water, driven by the electrostatic interactions between the charged end groups. The antiparallel orientation is observed at distances [*0.4-0.*6]nm between the centers of mass of FF. Similar observation has also been reported in a previous simulation study based on a coarse grained model[23]. Note that for smaller distances, about 0.2-0.3nm (data not shown here), the molecules prefer a normal orientation in order to reduce the very strong repulsive interactions. As the distance between the centers of mass of the two peptides increases, the electrostatic interactions between the charged end groups push the molecules to a parallel orientation, which is feasible since there is enough space between them for this conformation. This is obvious in Figure 5a at the distance of *1.0nm*, while the *0.8nm* distance is an intermediate conformation. These orientations are in favor of the formation of head-to-tail hydrogen bonds between FF peptides. In order to further study the role of the hydrogen bonds on the preferred orientation, we have also calculated the mean number of hydrogen bonds between FF molecules, for various values of θ angle. These numbers have been found similar for the different orientations; i.e. the formation of hydrogen bonds does not lead to a specific orientation. A more detailed analysis of hydrogen bonds will be presented in the following section. Finally note that there isn't any preferable orientation between FF peptides in methanol, for all distances, except for a short one, *0.4nm*, where an almost vertical orientation is preferred due to the strong repulsive interactions. The reason for the different orientations of the peptides, in aqueous

and in methanol solutions, is the slight difference in terminal groups of FF in the two solvents, i.e. end FF groups are not charged when FF is dissolved in methanol.

c) Hydrogen Bonds

In the previous section we used the pair radial distribution function as a measure of self-assembly of FF peptides in methanol and in water. This description is based on the molecular level, while a more detailed analysis, in atomic level, can be the number of hydrogen bonds which are formed in both systems. The most common way to characterize a hydrogen bond is to consider a geometric criterion. There is a large variety of geometrical criteria involving interatomic distances and angles[39]. In this study we use a standard geometric criterion originally used to investigate hydrogen bond networks in pure methanol solutions[40,41]. According to this, a hydrogen bond exists if three geometric conditions are satisfied simultaneously: $r(\text{A...B}) \leq 3.5\text{Å}$, $r(\text{A...H}) \leq 2.6\text{Å}$ and $angle(\text{A...B-H}) \leq 30^0$, where A and B are the electronegative atoms (i.e., N and O in our system) and H is the hydrogen.

As a test case, we encountered the number of hydrogen bonds which are formed between solvent molecules (i.e., water-water and methanol-methanol) in the solutions of FF in water and FF in methanol correspondingly. The calculated values were *3.44* for water and *1.87* for methanol which are in the range of the bulk values, as they have calculated from various geometrical criteria[39,41]. In order to estimate the degree of destruction of the network of hydrogen bonds, that FF peptides cause to each solvent, we followed the following procedure. First we counted the hydrogen bonds between all FF molecules. Then we considered a sphere of radius equal to *1nm* around the center of mass

of each FF molecule and for the number of solvent molecules which lie in this region (i.e. creation of a list), we counted the number of hydrogen bonds, which are formed between the FF and solvent molecules, and the number of hydrogen bonds between solvent molecules of the list, taking into account the boundaries' contribution. Table 2 contains the corresponding results. The second column of Table 2 is the average number of hydrogen bonds per FF molecule (or per solvent molecule for the last two lines); while the two next columns show the average number of hydrogen bonds, which are formed within (intramolecular) and between (intermolecular) FF molecules respectively. The last column contains the fraction of FF molecules which participate in more than one hydrogen bonds with other FF or solvent molecules in the list. Note that the data are independent of the radius of the sphere, as far as this radius is larger than about $2R_g$. Table's values show: (a) a larger number of hydrogen bonds between FF peptides in water solution in contrast to methanol solution. This result is in agreement with the self-assembly picture of FF in water. (b) Moreover, a remarkable observation is the existence of intramolecular hydrogen bonds in both solvents. They consist the *21.8%* of the total hydrogen bonds between FF peptides in water, whereas, in methanol this percentage is even higher, of the order of *74.6%*. This is indicative of a tendency of FF molecules to attain "folded" structures, especially in methanol. (c) Another interesting point is that almost all FF molecules participate in multiple hydrogen bonds with solvent molecules. In water the percentage is *99.9%* and in methanol *99.2%*. The corresponding percentage for FF molecules which participate in multiple hydrogen bonds with other FF molecules is *10.4%* in water and *8.2%* in methanol. (d) Finally, there is a clear difference concerning the number of hydrogen bonds (per solvent molecule) of solvent molecules,

within the sphere, between water and methanol: For water molecules this number (*2.44*) is smaller than the corresponding bulk water value (*3.44*), whereas for methanol it is (*1.81*) very close to the bulk methanol value (*1.87*). The above numbers also provide a consistent quantitative evidence for the higher degree of disturbance of the hydrogen bonds network of water in FF/water mixtures, compared to methanol in FF/methanol systems.

In order to further quantify the role of hydrogen bonds, we calculate the mean number of solvent molecules which are contained in the sphere of *1nm* radius, around one FF molecule; this is *83.13* for water and *52.44* for methanol. The total number of hydrogen bonds around one FF in water is *2.44*83.13+8.32=211.16* though, for *83.13* molecules of pure water this number would be equal to *3.44*83.13=285.97*, which means an *26.2%* decrease of water hydrogen bonds due to the presence of FF. The analogous calculation in methanol gives *1.81*52.44+4.41=99.33* total hydrogen bonds around one FF in methanol and *1.87*52.44=98.06* for *52.44* molecules of pure methanol. The difference is within the statistical uncertainty and shows that, in this case, the network of hydrogen bonds is almost unaffected by the presence of FF. The above calculations reflect the degree of destruction of hydrogen bonds network in the two solvents and it is obvious that the destruction is much stronger in water. Based on this observation, formation of hydrogen bonds could be considered as a driving force for self assembly.

Intramolecular hydrogen bonds between FF peptides can be thought as an important factor which induces the dissimilarities in the hydrogen bond networks. The *74.6%* of the total hydrogen bonds, which have been detected in methanol solutions, is the intramolecular hydrogen bonds and more specifically, hydrogen bonds between the

terminal ends of FF molecules. The small amount of intermolecular hydrogen bonds between FF peptides in methanol is indicative of the absence of self-assembly. On the other hand, intramolecular hydrogen bonds consist only the *21.8%* of the total number of hydrogen bonds between FF peptides in water, while the rest *78.2%* are the intermolecular hydrogen bonds which support the self assembly scenario in aqueous solutions.

Moreover, the charged terminal ends of FF in water lead to head-to-tail (intermolecular) hydrogen bonds between FF molecules, involving the peptide termini. According to x-ray measurements of Gorbitz et al.[8,9] and of Kim et al.[42], these head-to-tail hydrogen bonds are very important for the peptide layer closure around the central water channel and therefore for nanotube formation. This will be further checked in a future work involving simulations of larger systems through coarse-grained models.

The strength of a hydrogen bond can be characterized by the distributions of the values of the variables used for its definition (i.e., geometrical criterion). Figures 6 and 7 contain these distributions for two distances and one angle in both solvents. Figure 6a-6d contains the values for *r*(A...B) and *r*(A...H), expressed in probabilities, for hydrogen bonds which are formed between FF molecules in both solvents. The distributions of the intramolecular and the intermolecular hydrogen bonds are presented separately, together with the total histogram. The corresponding probabilities for hydrogen bonds which are formed between FF-solvent molecules and for the *angle*(A...B-H), are depicted in Figure 7a -7d.

A comparison of the curves between Figures 6a and 6b for *r*(A...B) and between 6c and 6d for *r*(A...H) correspondingly, concludes that, although the hydrogen bonds

which are formed between FF molecules in methanol are fewer, than the ones in water, they seem to be stronger, given that they are formed at shorter distances. In aqueous solutions, intramolecular hydrogen bonds tend to be formed at longer distances because the donor and the acceptor atoms are not fully flexible to approach each other very closely. This is due to two reasons; the one is that they are bonded in the same molecule, while the other is the lack of space because of self-assembled structures. However, the self-assembled structures favor the formation of intermolecular hydrogen bonds. On the other hand, in methanol solutions, intramolecular hydrogen bonds can be formed at shorter distances compared to aqueous solutions, because the molecule has enough space to form more compact folded structures, since there are not other molecules in its vicinity. In this case, intermolecular hydrogen bonds are substantially fewer and weaker, because FF peptides do not prefer to come close to one another. All these observations are reflected in the total histograms, which have been constructed from the whole number of hydrogen bonds and render hydrogen bonds in methanol stronger than the ones in water.

The probabilities of the distances for FF-solvent hydrogen bonds and the probabilities of θ – values, over which hydrogen bonds are formed, for all cases (i.e., FF-FF and FF-solvent) are depicted in Figure 7a-7d. These histograms are almost the same in both solvents, within the statistical accuracy.

Finally, the values for r(A...H) distances from our calculations (Figure 6c) are in good agreement with experimental reported values for hydrogen bonds between FF-FF pairs in water, for the case of nanotubes formation[42].

d) Characterization of aggregates as a function of temperature

Another interesting aspect concerns the effect of temperature on the structure of FF peptides in water and in methanol. For this reason a series of replica exchange molecular dynamics simulations have been performed for two systems of FF (systems 5 and 6) covering a temperature range of about *50K*: [*295 – 342.74*] *K* for FF in water and [*285 – 331.12*] *K* for FF in methanol.

Starting with structure, the pair radial distribution function between FF molecules (FF-FF) is presented in Figure 8, for three different temperatures (the lowest, the middle and the highest value) for both solvents. A characteristic decrease of the value of the first peak of rdf and an increase of the values of the tail with temperature is observed for FF in water (Figure 8a). This is a prospective behavior since, as temperature increases, FF molecules become more mobile, and consequently the self assembled structures less stable. Nevertheless, even at high temperatures, self assembled conformations of FF dominate in water solution. On the other hand, there is not any observable change in the shape of rdf curve for FF in methanol at the three different temperatures (Figure 8b). The order of structure is substantially less in methanol compared to water and it seems to be unaffected of temperature.

Moreover, the radius of gyration of FF molecules in water and in methanol, in the whole range of temperatures of the replica exchange runs, has been calculated. We found that R_g values remain constant at all temperatures studied here, which means that the size of FF peptides is independent of temperature in both solvents.

Interesting information for the structures, which are formed from FF peptides, in water and in methanol, is the size of the aggregates and the number of peptides which

participate in these structures. Both of these quantities have been calculated and the way that they are affected by temperature has been examined.

Aggregates are structures which are created and destroyed during the simulation and their size varies (i.e., number of FF that they contain), depending on temperature, because temperature rise induces larger energy fluctuations. In order to characterize an aggregate, we propose a definition of a quantity, similar to the radius of gyration of a single molecule. In the present case this quantity can be thought as an effective "radius of gyration", (R_g^{eff}), and is based on the calculation of the center of mass of all FF peptides in our system, taking into account system's periodicity (i.e., minimum image convention). The effective radius of gyration, R_g^{eff} , of a cluster is a measure of the size of all FF molecules, even if no aggregates exist, because it takes into account the position of all FF peptides, either they have self assembled or not. Using the position of the center of mass we applied the formula for R_g, where, the smaller the value of R_g^{eff} the more FF peptides constitute the aggregate. For a homogeneous FF/water system (where aggregates do not exist) a simple calculation leads to a result for the R_g^{eff} equal to the half of the simulation box (i.e., the distribution of R_g^{eff} is a δ-function around the center of the simulation box).

The distributions of the R_g^{eff} 's values at four different temperatures are presented in Figure 9. Figure 9a and 9b depict the results for FF in water and in methanol respectively. In water solutions the peak of the curves is moved to higher values as temperature increases, which indicates aggregates of fewer FF. This observation is

consistent with the rdf behavior as a function of temperature. Although temperature increase moves R_g^{eff} curve to higher values, it is fairly below the middle of the simulation box, (*6/2*)nm, even at the highest temperature, while a considerable part of the curve lies at very small values. This picture shows that self assembly is present at any temperature in water, though at high temperature values, energy fluctuations slow down aggregate's formation through the very frequent transition among different cases of aggregates of smaller size. R_g^{eff} distribution is very characteristic in methanol, where for all four temperatures the curves are similar, they have small width and they are centered at a value slightly lower than the half of the simulation box, (*6/2*)nm. This result is again in agreement with the features of rdf curves and corroborates the inexistence of self assembly of FF in methanol.

Next, based on the above procedure the number of FF peptides in an aggregate can be calculated. We consider a spherical shell of an arbitrary radius of *2nm* around the calculated center of mass of the FF molecules and count the number of peptides whose center of mass lies in this region. Then the average number over all the configurations is calculated. For a uniformly distributed solution a simple calculation gives that the number of molecules which lie in a sphere of radius equal to *2nm* is almost *2.5*, (i.e, for simulation box *L=6nm* and total number of FF molecules in the solution equal to *16*: $\frac{16}{L^3} = \frac{N}{\left(\frac{4}{3}\pi R_c^3\right)} \Rightarrow N = 2.48$). In Figure 10a the average number of FF peptides in the spherical shell is presented as a function of temperature for FF in water and FF in methanol. In water solution this number is a decreasing function of temperature, however

at all temperatures it is a high percentage of the total number of FF molecules in the solution, between *66%-90%*. On the contrary, in methanol this number is around *4* at all temperatures.

An estimation of the stability of the structures, which are formed in the two solvents, as temperature increases, is given by the distribution of the number of FF peptides in an aggregate which is depicted in Figures 10b and 10c. As temperature increases the distribution becomes broader in water (Figure 10b), which reflects the enhancement of energy fluctuations. At the highest temperature (*342.74K*) a two peak distribution is presented, which means that two different sizes of aggregates are dominant in the solution and there is a continuous transition between them. In methanol (Figure 10c), although the structure is substantially less, it seems to have a constant order which is unaffected by temperature. These observations are in accordance with the previous discussion and corroborate our results.

IV. Experimental Results

In order to correlate the theoretical results with the corresponding experimental conditions, the following experiments were carried out: the FF peptide powder was dissolved in water or methanol by heating and sonication at 55^oC. It was subsequently transferred to 27^oC in order to induce self-assembly. These conditions were chosen in order to ensure maximum compatibility between the modeling and experimental systems. The FF water sample incubated in 55^oC remains clear during incubation at 55^oC, while

following its transfer from 55^oC to 27^oC, the sample instantly becomes turbid due to the formation of needle-like structures in solution that are visible with the naked eye (Figure 11). The methanol samples do not show any visible structure formation in both temperatures and there is not any change in turbidity as a function of the incubation time, even after two hours of incubation. Therefore, the self-assembly propensity in methanol seems to be much weaker than in water.

We subsequently sought to test the self-assembly propensity upon evaporation on glass slide surfaces. Figures 12a and 12b show SEM pictures of samples taken and dried on glass slides at ambient temperatures from vials incubated in both solvents in the following conditions: at time zero and after two hour incubation at 55^oC respectively. The FF peptides incubated in water formed straight, well-defined fibers and/or tubes both at time zero and after two hour incubation at 55^oC. For the methanol samples, dendritic- like structures are observed, rather than uniform and well-defined fibers and tubes.

Figures 13a and 13b show SEM pictures of samples taken and dried on glass slides from vials at time zero and two hours following transfer from 55^oC to 27^oC. Well-defined, straight fibers and tubes are again observed in the water samples for both incubation times. For the methanol samples, dendritic-like structures are observed that occasionally co-exist with amorphous peptide "films" on parts of the glass surface. In summary, the FF peptide efficiently self-assembles in solution in aqueous conditions upon transfer from 55^oC to 27^oC. In methanol, no visible self-assembly is observed in solution. All samples show structure formation upon evaporation on glass slides. While the structures formed out of aqueous solutions display well-defined tuber/fiber morphologies, the structures formed out of methanol show less well-defined dendritic

and/or film morphologies. We attribute the latter structures as metastable not equilibrium structures formed during the evaporation of the solvent.

V. Discussion and Conclusions

We have studied the self-assembly of dialanine (AA) and diphenylalanine (FF) in different solvents through detailed all-atom, explicit solvent, simulations and experiments. An aqueous (H_2O) and an organic (CH_3OH) solvent were studied. Clear evidence for the self-assembly of FF in water was found from both simulations and experiments. On the contrast absence of self assembled FF structures in methanol was observed.

The potential of mean force (PMF) between two FF molecules (Figure 2b) constitutes the first evidence for the self assembly of FF in water and not in methanol. There is a clear attractive part in the PMF curve for water solution whereas, for methanol solution PMF is totally repulsive. This finding is further confirmed from the direct calculation of the pair radial distribution functions between FF molecules (FF-FF) and between FF-solvent (FF-W / FF-M) molecules for both solvents (Figure 3). There is an obvious attraction of FF in water which leads to the formation of aggregates in contrast to methanol solution. Furthermore an optical observation of snapshots of FF in water and in methanol (Figure 4) supports our conclusion. In addition, the radius of gyration of a single peptide, which is a measure of its mean size in a solution ($<R_g>$), is found to be

slightly larger for FF in methanol than in water, which renders methanol a rather better solvent for FF.

Experimental observations, which can be classified in two kinds, the optical ones (Figure 11) and the SEM pictures (Figure 12 and 13) are in qualitative agreement with these findings. Vials of Figure 11 are totally transparent for methanol solutions in all four instants. Pictures are identical for both high ($55\ ^oC$) and low ($27\ ^oC$) temperature values and are independent of time as well. Simulation results for this system lead to exactly the same conclusion as it is presented in Figures 2b, 3b, 4b and 8b and corroborated by whole analysis throughout the paper.

On the other hand, in water solutions samples become turbid immediately upon transfer from $55\ ^oC$ to $27\ ^oC$, which indicates the very rapid formation of self-assembled structures from FF peptides. There is a clear difference in pictures between $27\ ^oC$ and 55^oC, where the turbidity is much more pronounced in the former case. These qualitative features are again confirmed by simulation results as presented in Figures 2b, 3a, 4a and 8a, which are the most representative ones.

SEM pictures of Figure 12 and 13 show the specific structures of FF formed upon evaporation from water and methanol for all four cases which correspond to vials of Figure 11. Fibers and tubes were detected in water for both temperatures that seem better defined at the lower value (27^oC). At 55^oC, the observed structures are formed upon evaporation of water, while at $27\ ^oC$, the observed structures must correspond to a mixture of pre-existing structures in solution plus additional structures formed upon evaporation. In methanol, although dendritic- like and amorphous structures were observed with SEM, the transparent vials lead to the assumption that these structures are

solely formed during the evaporation of the solvent. Calculation of corresponding measures, for the characterization of the shape of the self assembled structures, is not possible in our simulation model, because of the limitations in systems' size, which is always a problem in atomistic simulations. These structures are macroscopic, of the order of a few *micrometers to millimeters*, which are not covered with atomistic models.

Atomistic simulations provide useful information for many unexplored issues, like the driving force of self assembly in a specific solvent or the structure and dynamics in the atomic level. Our simulation work constitutes an extensive study of the above issues for FF in water and in methanol.

The arrangement of FF peptides in the self assembled structures in water, was found to be in an antiparallel orientation, for short intermolecular distances, while as the distance increases FF peptides are settled gradually in a parallel orientation. This is a result of the electrostatic interactions between the charged end groups. For methanol solutions the orientation is random at any distance.

Furthermore, the number of hydrogen bonds which are formed between FF peptides and FF-solvent molecules can be considered as a measure of self assembly in atomic level. We have encountered hydrogen bonds in both solvents and found that the number of hydrogen bonds between FF molecules is higher in water than in methanol. Moreover, the number of hydrogen bonds between FF and solvent is almost two times higher in aqueous solution compared to methanol solution. Using these numbers and based on a simple calculation for the degree of destruction of the hydrogen bonds network due to the presence of FF in both solvents, we show that hydrogen bonds constitute the major driving force for self assembly.

The effect of temperature on the aggregate's formation was also explored through a series of replica exchange runs in a range of temperatures of about *50K*, for both solvents. Our results indicated attenuation of structure with temperature in the aqueous solution, something which is in qualitative agreement with the experimental observations, as it was mentioned above as well. We characterized aggregates as a function of temperature and found that temperature increase leads to smaller aggregates, where fewer FF peptides participate. In methanol, structure is almost unaffected by temperature in accordance also to experimental pictures. Furthermore the size of FF molecules seem to be unaffected by temperature in both solvents.

Finally, special mention must be done on the difference between FF and AA peptides. Although for AA the tendencies in all observations are the same as the ones which stand for FF in the corresponding solvent, the differences between the two solvents are substantially smaller. Starting from the potential of mean force (Figure 2a), we observe that it is totally repulsive for AA in methanol, while it has an attractive well for AA in water. This attraction is also reflected in structures, as they are presented in the pair radial distribution functions of AA-AA (Figure 3a and 3b). In methanol solution rdf curve is less structured than the one in water. Nevertheless, the differences between the two solvents are much more pronounced in FF solutions. These observations lead to the conclusion that phenyl rings are responsible for the stronger attraction which is observed in FF aqueous solutions. This confirms the critical role postulated and experimentally observed for the phenylalanine residues in amyloid self assembly[12,13]. On the other hand, phenyl rings do not seem to affect the structure in methanol solutions.

Current work concerns application of the whole methodology in FF peptides modulated by N-termini blocking or conjugated to other chemical moieties[43], as well as implementation of coarse-grained models for the study of larger more realistic systems[44].

Acknowledgements

The authors would like to thank Maria Vamvakaki and Thanasis Koutsolelos for useful discussions. This work was partially supported by the European Union's Seventh Framework Programme (FP7 REGPOT-2009-1) project ''Archimedes Center for Modeling, Analysis and Computation'' under grant agreement n 245749 as well as by the European Union (European Social Fund - ESF) and Greek national funds through the Operational Program "Education and Lifelong Learning" of the National Strategic Reference Framework (NSRF) - Research Funding Program: THALES.

System	Name	N-peptide	N-solvent	#atoms	T(K)
1	AA in Water	16	3696	11328	300
2	AA in Methanol	16	1632	5120	300
3	FF in Water	16	6840	21112	300
4	FF in Methanol	16	3024	9648	300
4 RE	FF in Water	16	6840	21112	295-343
5 RE	FF in Methanol	16	3024	9648	285-332

Table 1.

Setup details for the simulated systems

Molecules	<HB>	Intra HB	Inter HB	Molec. in Multiple HB
FF-FF/FF in H_2O	0.36	0.077	0.278	0.104
FF-FF/FF in CH_3OH	0.20	0.150	0.051	8.21E-02
$(FF\text{-}W/FF)_{List}$	8.32			0.999
$(FF\text{-}M/FF)_{List}$	4.41			0.992
$(W\text{-}W/W)_{List}$	2.44			-
$(M\text{-}M/M)_{List}$	1.81			-
$(W\text{-}W)_{Bulk}$	3.44	-		-
$(M\text{-}M)_{Bulk}$	1.87	-		-

Table 2.

Average number of hydrogen bonds between FF-FF, FF-Solvent and Solvent-Solvent molecules (water ≡ W and methanol ≡ M) for FF in water and FF in methanol at *c=0.0385grFF/cm^{3}solvent*. Error bars are about 1% of the actual values.

Figure 1. Atomistic structure of diphenylalanine in water **(a)** and in methanol **(b)**.

Figure 2. The potential of mean force (PMF) as a function of distance between the centers of mass of **(a)** AA in water (closed symbols) and in methanol (open symbols), **(b)** FF in water (closed symbols) and in methanol (open symbols). Solid horizontal lines correspond to k_BT, thermal energy.

Figure 3. The pair radial distribution function (rdf) calculated for the cm of peptides: FF-FF (thin lines) and AA-AA (thick lines) **(a)** in water and **(b)** in methanol, **(c)** FF-Water (thin line) and FF-Methanol (thick line), at *T=300K* and $c=0.0385 grFF/cm^3 solvent$.

Figure 4. Snapshots from MD simulations of a solution of FF in **(a)** water and **(b)** methanol at *T=300K* and $c=0.0385 grFF/cm^3 solvent.$

Figure 5. Probable orientations between a pair of FF peptides in **(a)** water and **(b)** methanol, in terms of angles between their end to end vectors, at different cm–cm constant distances (*Dr*).

Figure 6. Distributions of the values of the two distances, used in the geometrical criterion, for hydrogen bonds: **(a)** FF-FF in water r(A…B); **(b)** FF-FF in methanol r(A…B); **(c)** FF-FF in water r(A…H); **(d)** FF-FF in methanol

r(A…H). The two contributions of the intermolecular and the intramolecular hydrogen bonds are depicted separately in all cases.

Figure 7. Distributions of the values of the two distances, used in the geometrical criterion, for hydrogen bonds: FF-water and FF-methanol **(a)** r(A…B); **(b)** r(A…H). Distributions of the values of the angle used in the geometrical criterion for hydrogen bonds: **(c)** θ for FF-FF in water and in methanol**; (d)** θ for FF-water and FF-methanol.

Figure 8. The pair radial distribution function (rdf) calculated for the cm of peptides at $c=0.0385grFF/cm^3solvent$: **(a)** FF-FF in water, at T=[*295, 316.39, 342.74*]K and **(b)** FF-FF in methanol, at T=[*285, 311.84, 331*.12]K.

Figure 9. Effective radius of gyration for the system of **(a)** FF in water, at T=[*295, 307.4 316.39, 342.74*]K and **(b)** FF in methanol, at T=[*285, 299.61, 311.84, 331*.12]K, at $c=0.0385grFF/cm^3solvent$

Figure 10. **(a)** Average number of FF molecules in an aggregate as a function of temperature at $c=0.0385grFF/cm^3solvent$ for FF in water and FF in methanol. Distribution of the number of FF molecules **(b)** in water and **(c)** in methanol, at different temperatures.

Figure 11: Photographs of peptide solutions after incubation in various conditions. In vials labelled with "A" the FF peptide is dissolved in water, whereas in vials labelled with "B", it is dissolved in methanol. **(a)** Left: Vials instantly after heating at 55^oC. **(a)** Right: Vials after two-hour incubation at 55^oC. **(b)** Left: Vials instantly after being transferred from 55^oC to 27^oC preincubated vials. **(b)** Right: Vials after two-hour incubation following transfer at 27^oC.

Figure 12: S.E.M. images of peptide samples following deposition of $10\ \mu L$ on glass slides and evaporation at ambient temperature. **(a)** Left: peptide structures in water instantly after heating at 55^oC. **(a)** Right: peptide structures in methanol instantly after heating at 55^oC. **(b)** Left: peptide structures formed on slides upon drying after two-hour incubation in water at 55^oC. **(b)** Right: peptide structures formed on slides upon drying after two-hour incubation in methanol at 55^oC.

Figure 13: S.E.M. images of peptide samples following deposition of $10\ \mu L$ solution on glass slides and evaporation at ambient temperature. **(a)** Left: peptide structures formed on slides upon drying of a solution incubated in water immediately following its transfer from 55^oC to 27^oC. **(a)** Right: peptide structures formed on slides upon drying of a solution incubated in methanol immediately following its transfer from 55^oC to 27^oC. **(b)** Left: peptide structures formed on slides upon drying of a solution incubated in water for two hours following its transfer from 55^oC to 27^oC. **(b)** Right: peptide

structures formed on slides upon drying of a solution incubated in methanol for two hours following its transfer from $55^{o}C$ to $27^{o}C$.

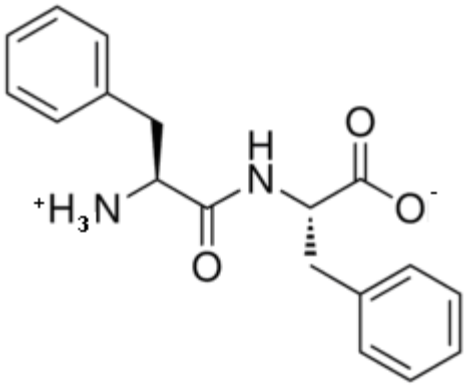

(a)

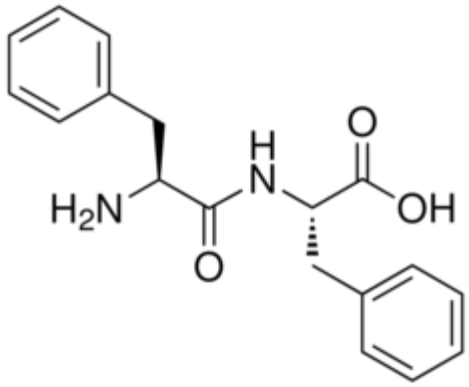

(b)

Figure 1

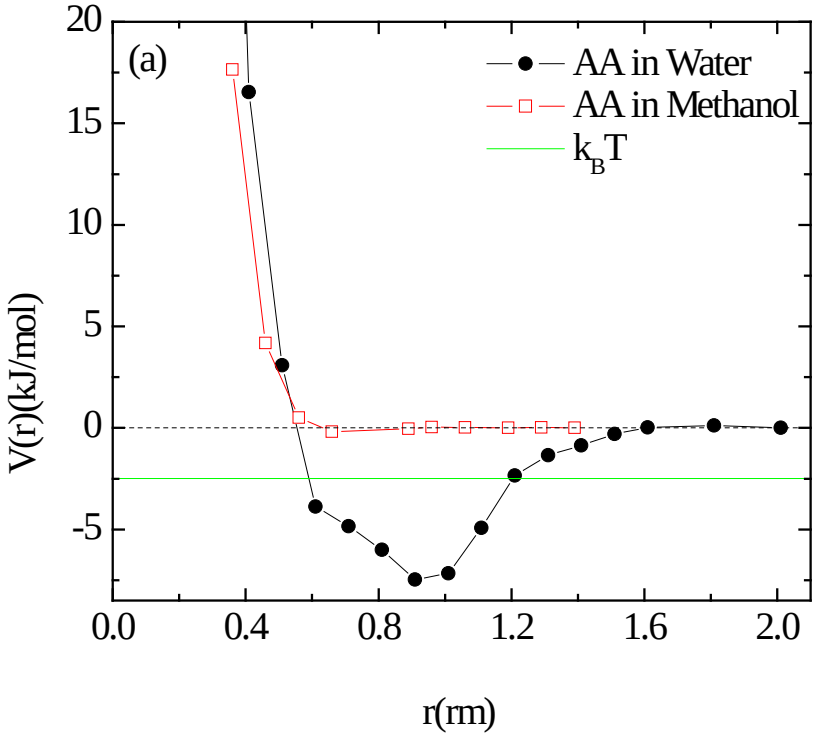
(a)
AA in Water
AA in Methanol
k_BT
V(r)(kJ/mol)
r(rm)
20
15
10
5
0
-5
0.0
0.4
0.8
1.2
1.6
2.0

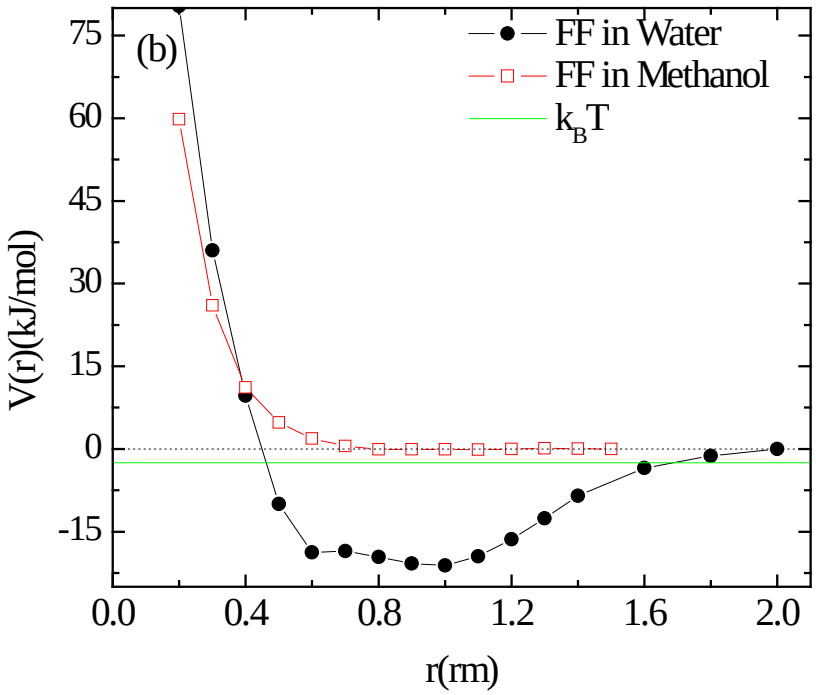
(b)
FF in Water
FF in Methanol
k_BT
V(r)(kJ/mol)
r(rm)
75
60
45
30
15
0
-15
0.0
0.4
0.8
1.2
1.6
2.0

Figure 2

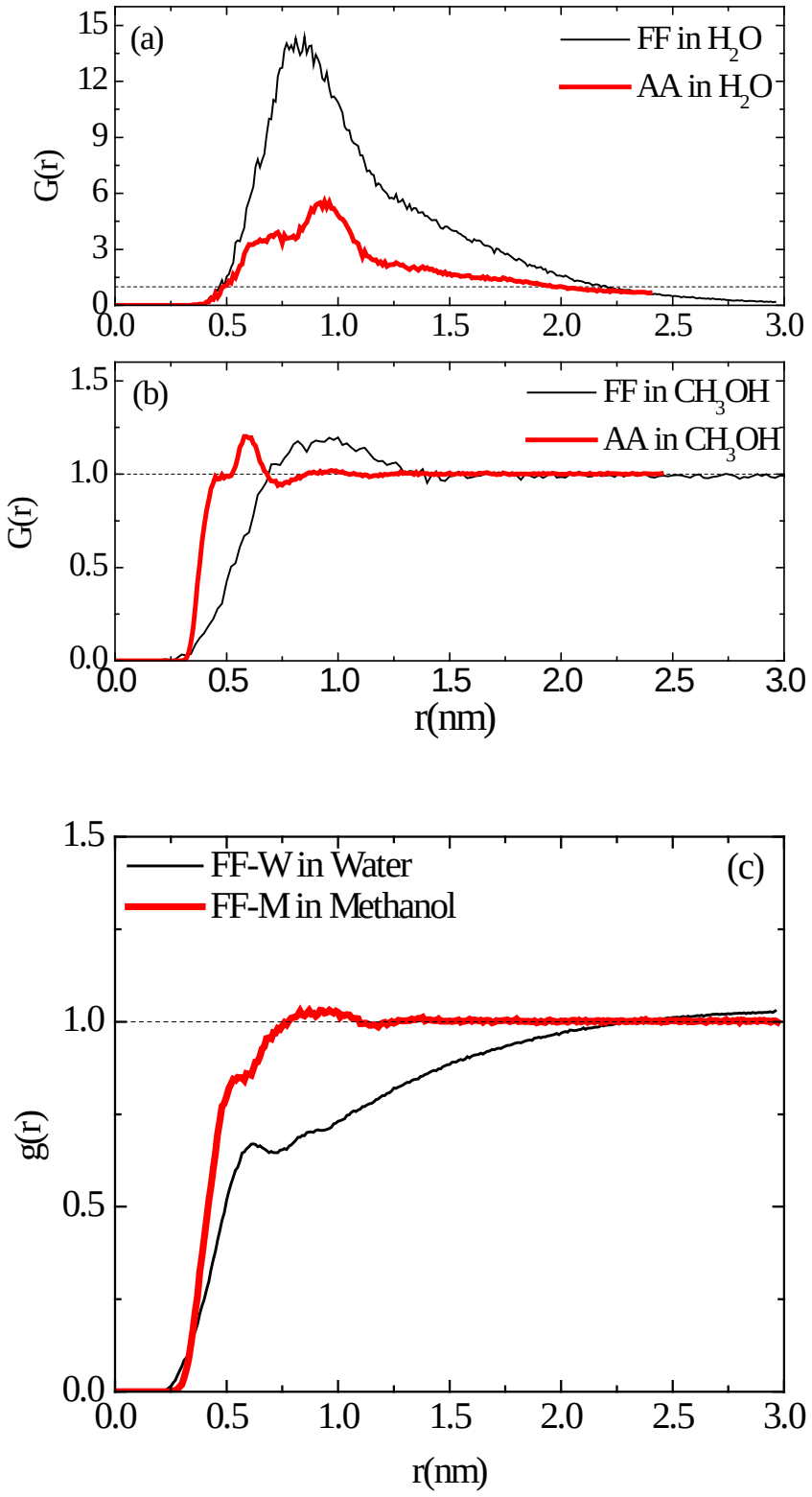
(a)
FF in H_2O
AA in H_2O
G(r)
15
12
9
6
3
0
0.0
0.5
1.0
1.5
2.0
2.5
3.0
(b)
FF in CH_3OH
AA in CH_3OH
G(r)
1.5
1.0
0.5
0.0
r(nm)
(c)
FF-W in Water
FF-M in Methanol
g(r)
1.5
1.0
0.5
0.0
r(nm)

Figure 3

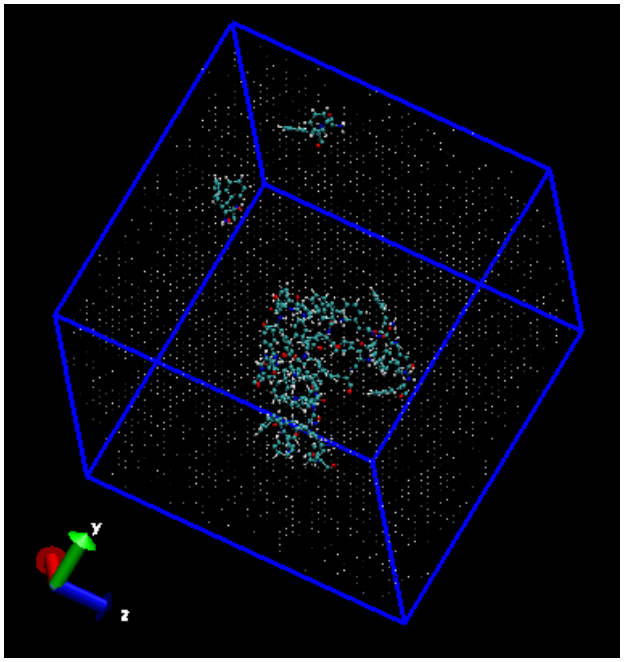

(a)

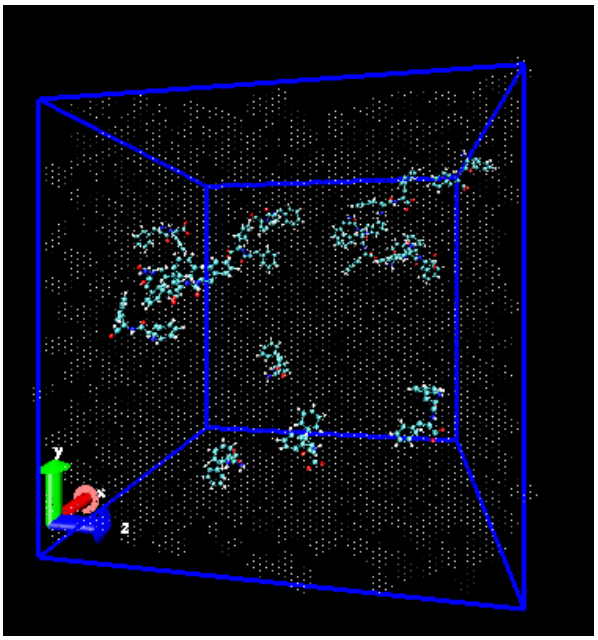

(b)

Figure 4

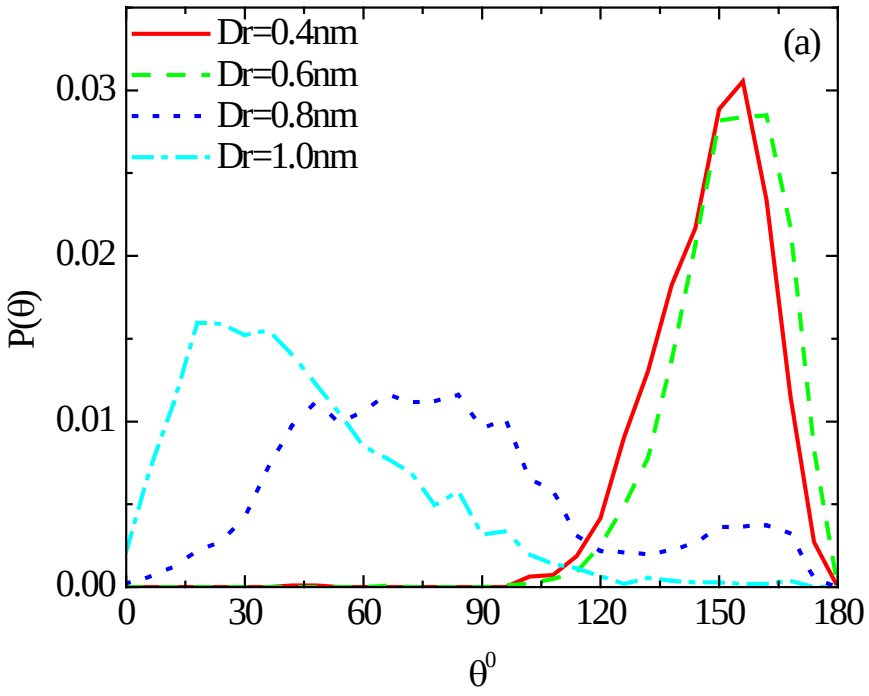
Dr=0.4nm
Dr=0.6nm
Dr=0.8nm
Dr=1.0nm
(a)
P(θ)
0.00
0.01
0.02
0.03
0
30
60
90
120
150
180
θ0

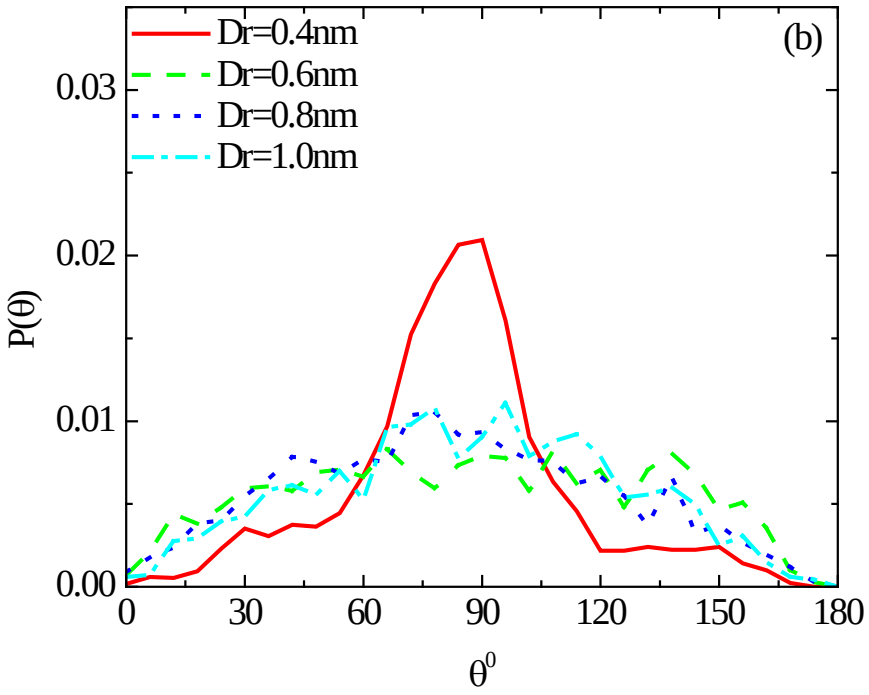
Dr=0.4nm
Dr=0.6nm
Dr=0.8nm
Dr=1.0nm
(b)
P(θ)
0.00
0.01
0.02
0.03
0
30
60
90
120
150
180
θ0

Figure 5

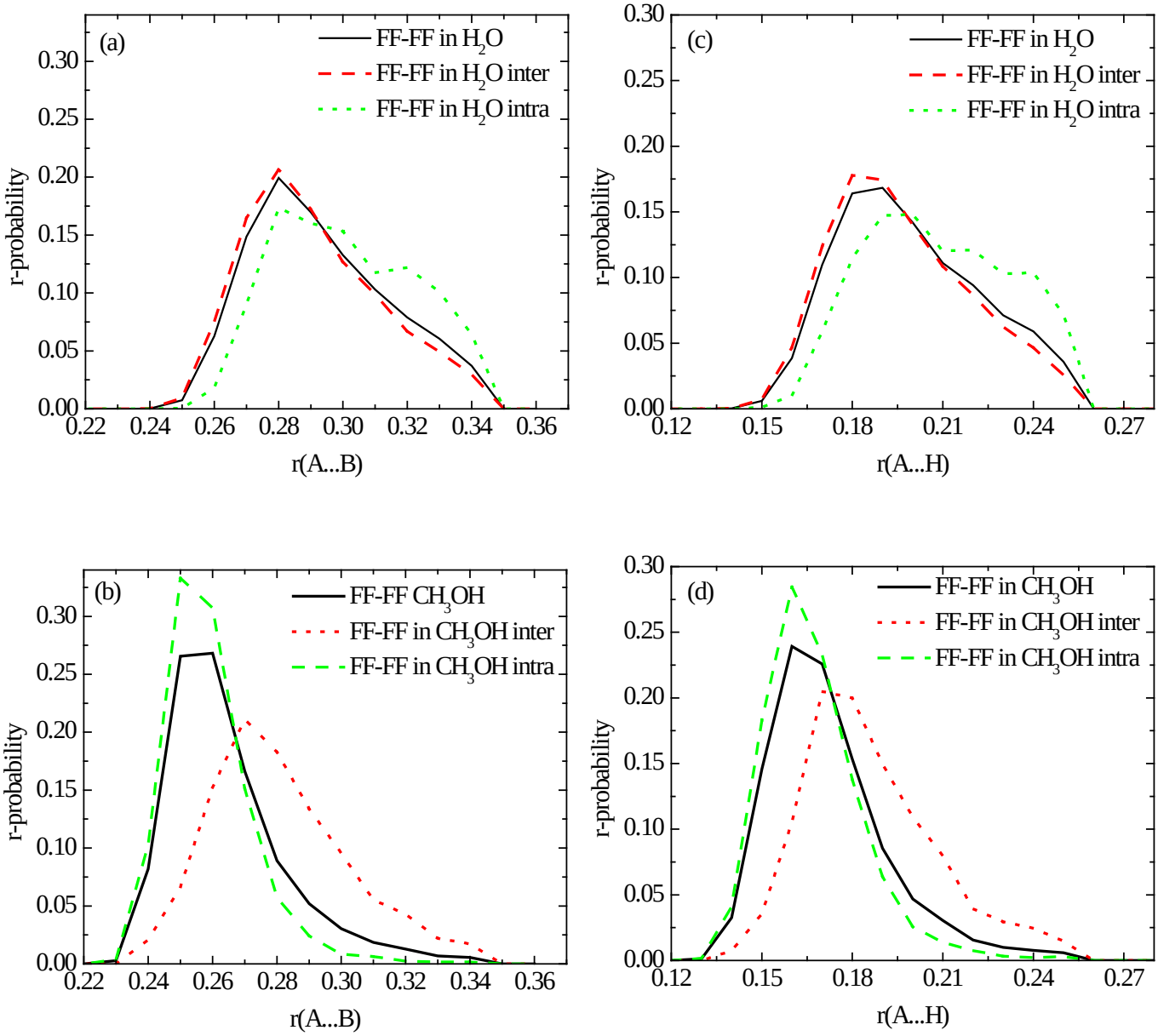
(a)
FF-FF in H2O
FF-FF in H2O inter
FF-FF in H2O intra
r-probability
r(A...B)
(c)
FF-FF in H2O
FF-FF in H2O inter
FF-FF in H2O intra
r-probability
r(A...H)
(b)
FF-FF CH3OH
FF-FF in CH3OH inter
FF-FF in CH3OH intra
r-probability
r(A...B)
(d)
FF-FF in CH3OH
FF-FF in CH3OH inter
FF-FF in CH3OH intra
r-probability
r(A...H)

Figure 6

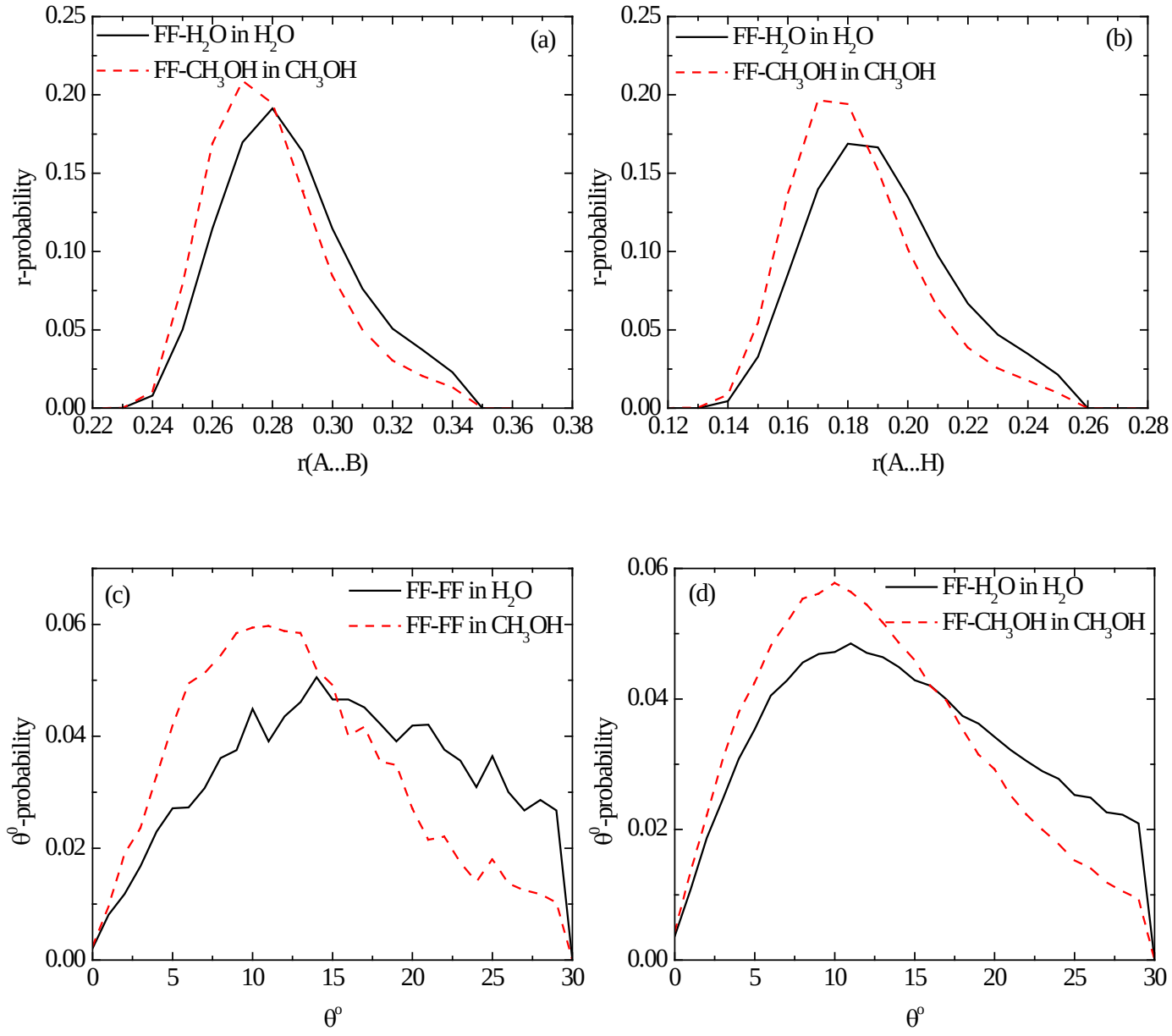
(a)
FF-H2O in H2O
FF-CH3OH in CH3OH
r-probability
r(A...B)
(b)
FF-H2O in H2O
FF-CH3OH in CH3OH
r-probability
r(A...H)
(c)
FF-FF in H2O
FF-FF in CH3OH
θ°-probability
θ°
(d)
FF-H2O in H2O
FF-CH3OH in CH3OH
θ°-probability
θ°

Figure 7

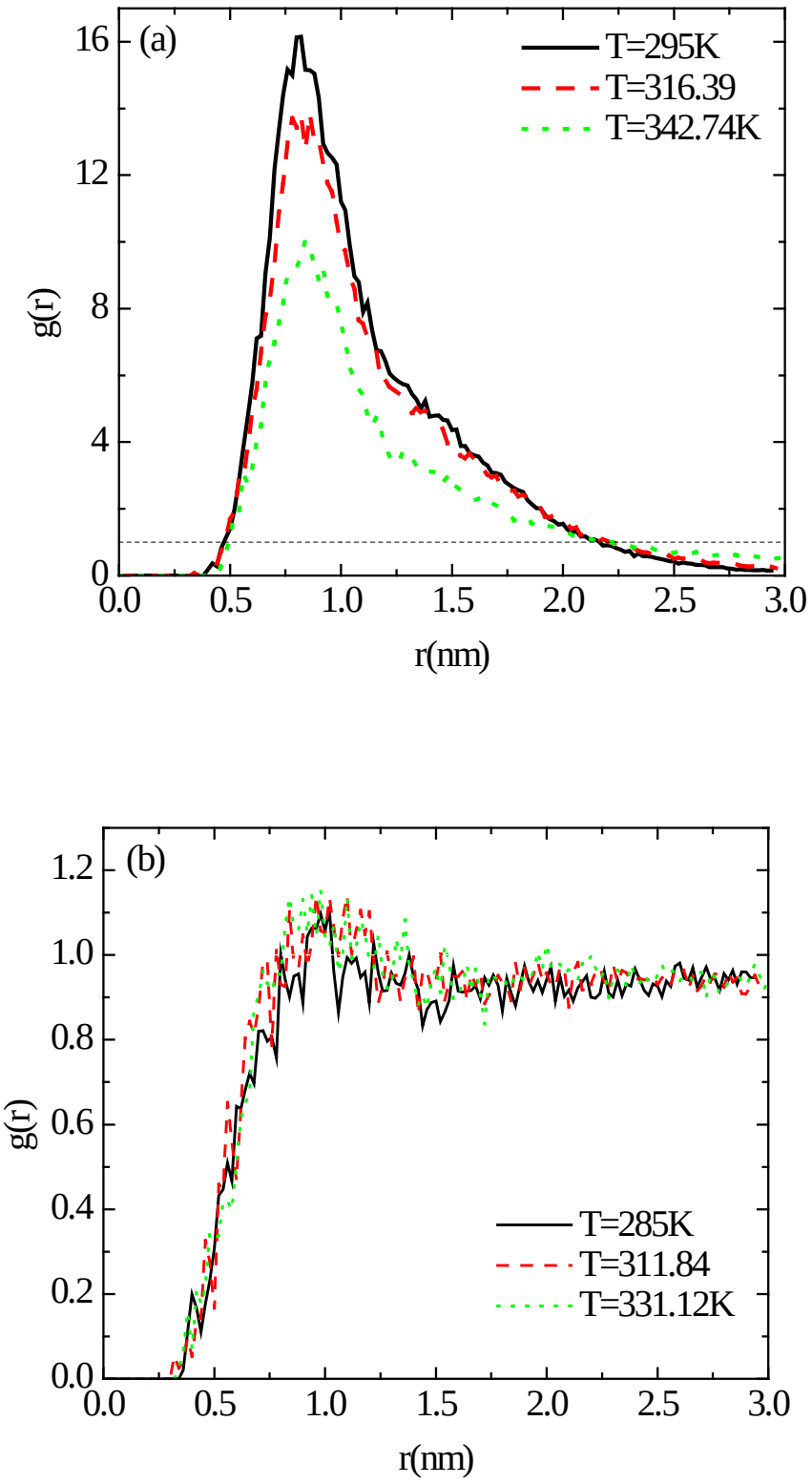
(a)
T=295K
T=316.39
T=342.74K
g(r)
r(nm)
0
4
8
12
16
0.0
0.5
1.0
1.5
2.0
2.5
3.0
(b)
T=285K
T=311.84
T=331.12K
g(r)
r(nm)
0.0
0.2
0.4
0.6
0.8
1.0
1.2

Figure 8

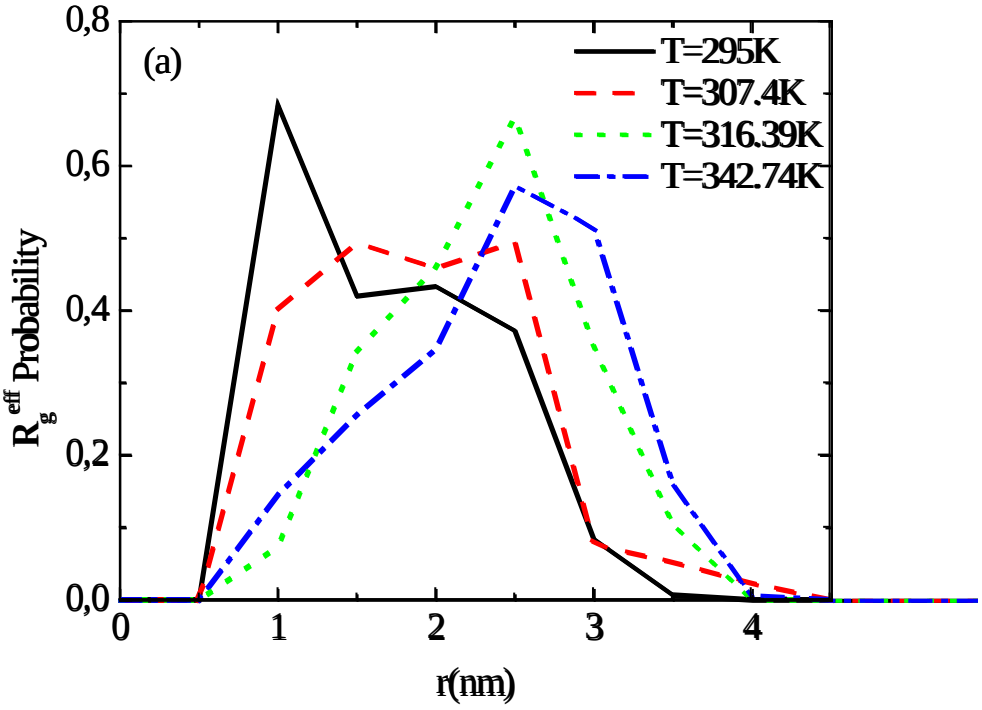
(a)
T=295K
T=307.4K
T=316.39K
T=342.74K
R_g^{eff} Probability
r(nm)
0,0
0,2
0,4
0,6
0,8
0
1
2
3
4

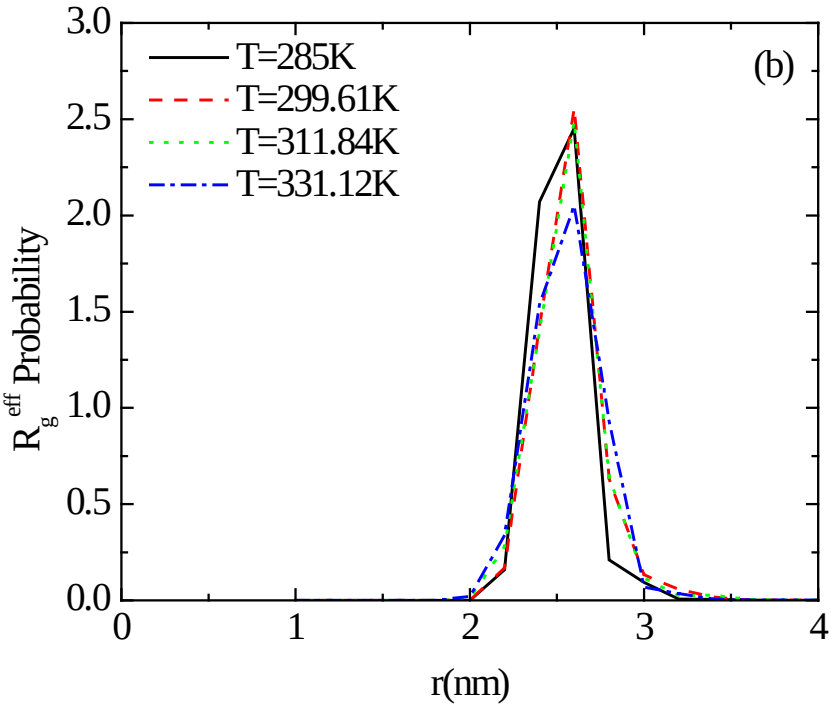
(b)
T=285K
T=299.61K
T=311.84K
T=331.12K
R_g^{eff} Probability
r(nm)
0.0
0.5
1.0
1.5
2.0
2.5
3.0
0
1
2
3
4

Figure 9

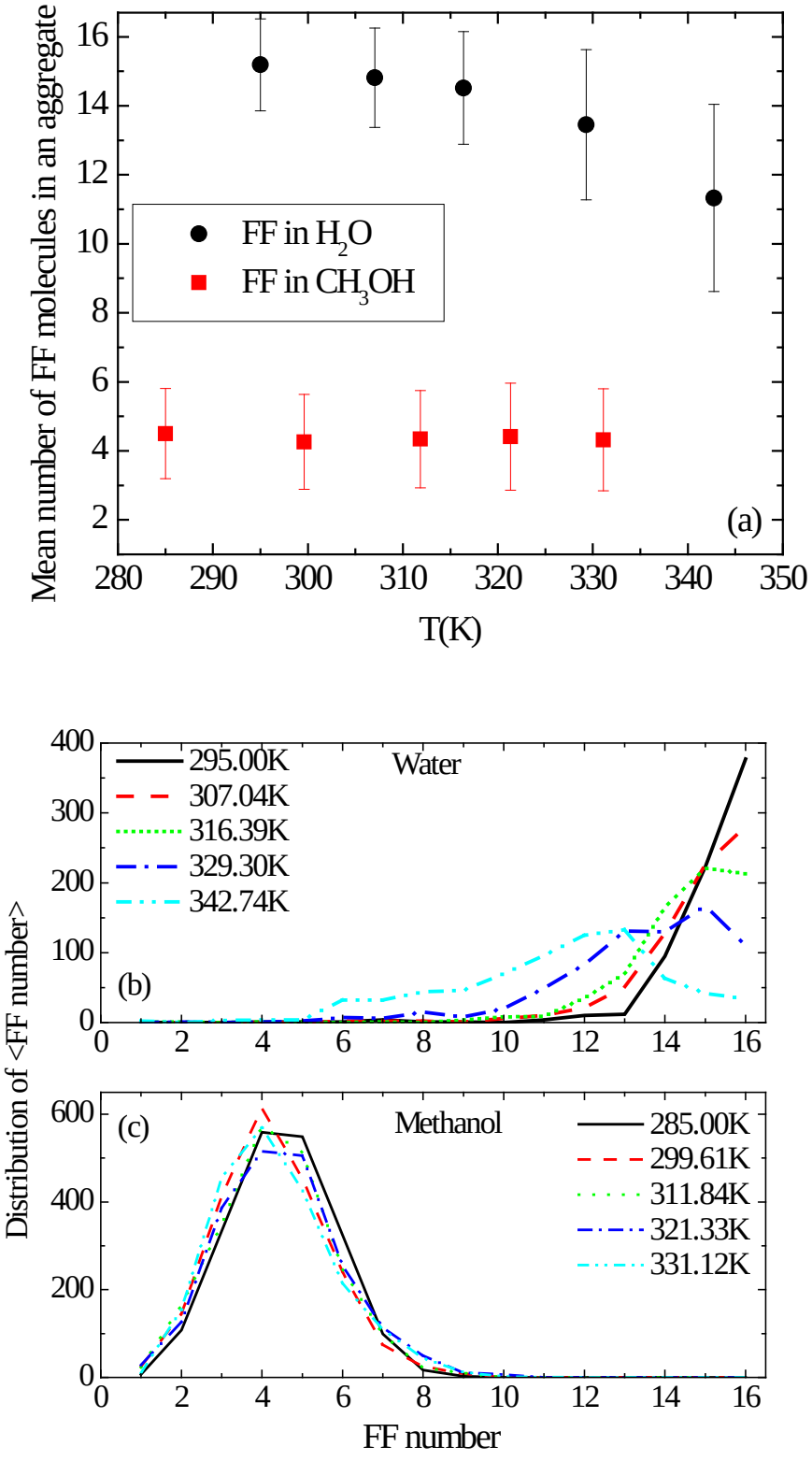
Mean number of FF molecules in an aggregate
T(K)
FF in H_2O
FF in CH_3OH
(a)
Distribution of <FF number>
Water
295.00K
307.04K
316.39K
329.30K
342.74K
(b)
Methanol
285.00K
299.61K
311.84K
321.33K
331.12K
(c)
FF number

Figure 10

(a)

(b)

Figure 11

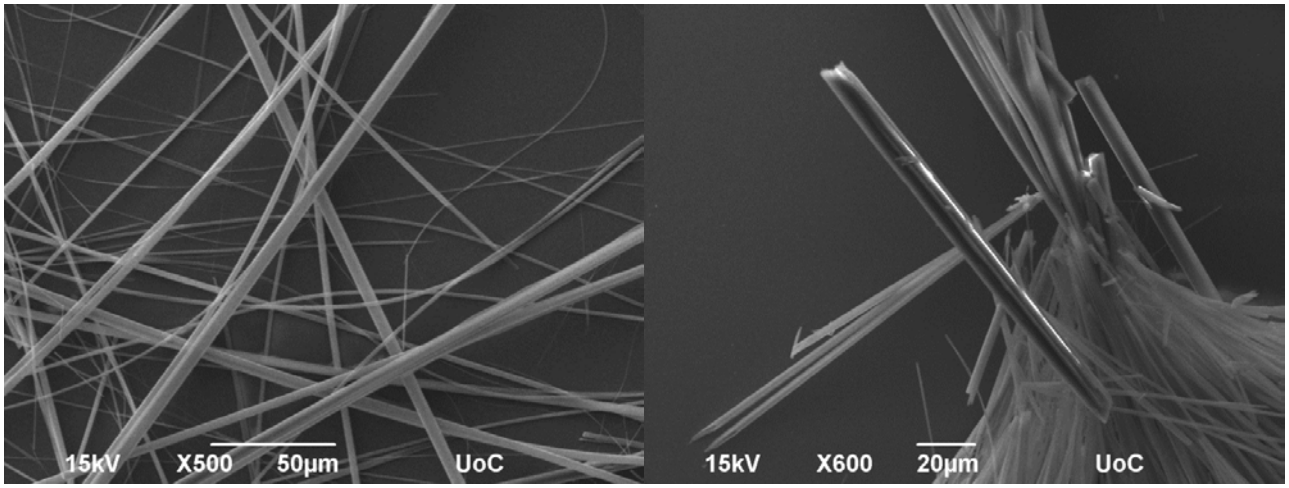
15kV X500 50µm UoC
15kV X600 20µm UoC

(a)

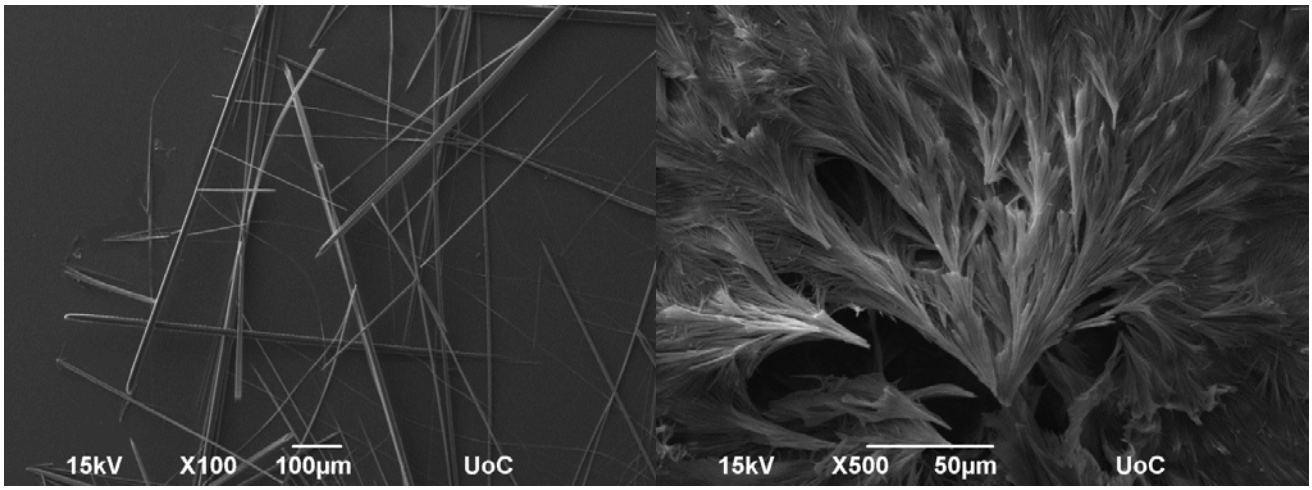
15kV X100 100µm UoC
15kV X500 50µm UoC

(b)

Figure 12

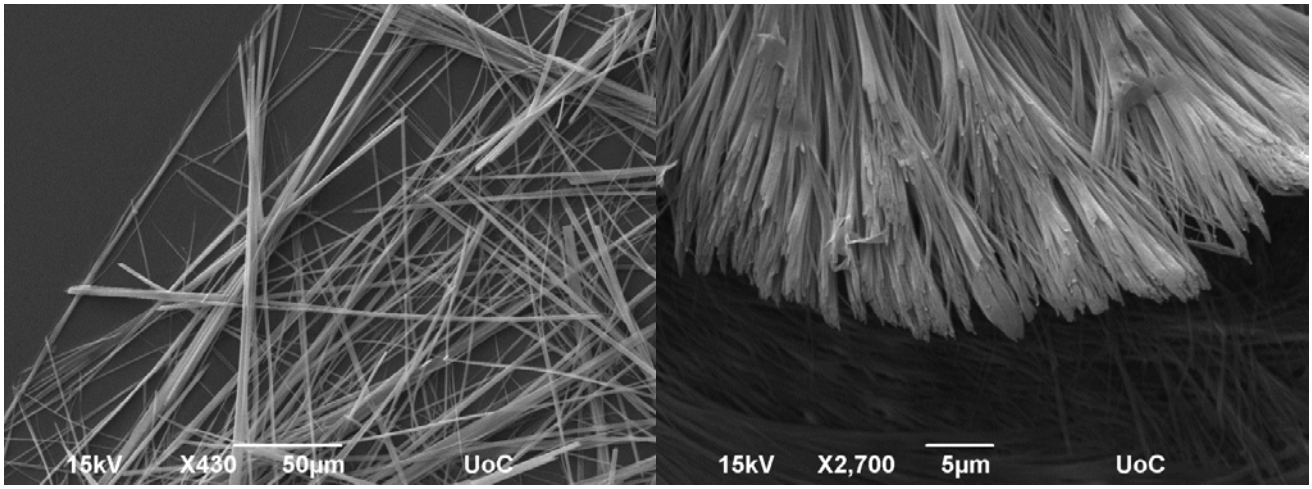
15kV X430 50µm UoC
15kV X2,700 5µm UoC

(a)

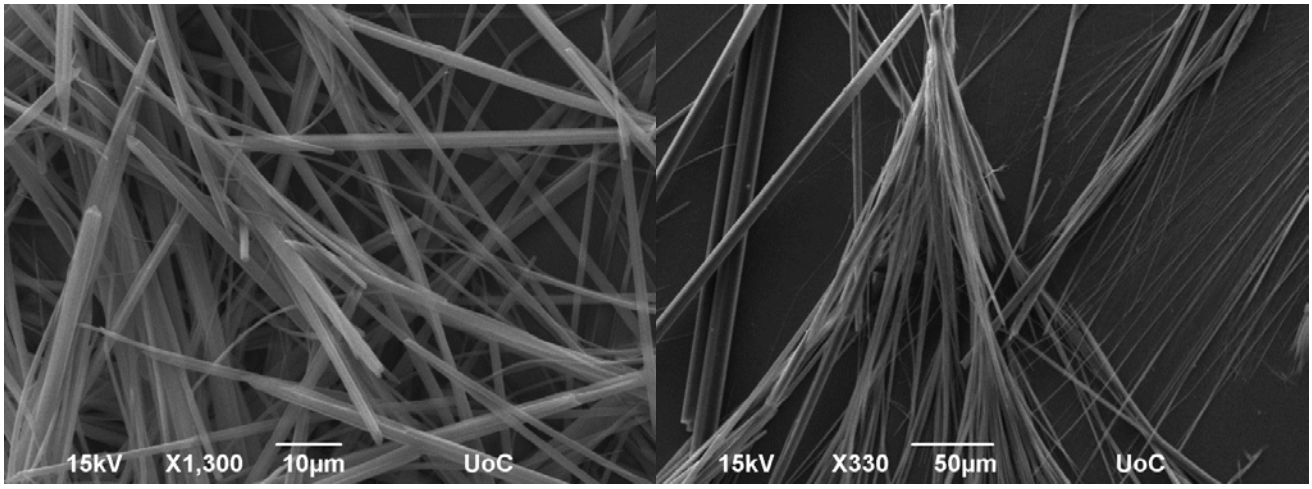
15kV X1,300 10µm UoC
15kV X330 50µm UoC

(b)

Figure 13

References

(1) Colombo, G.; Soto, P.; Gazit, E. *Trends Biotechnol*., **2007,** *25*, 211-218.

(2) Knowles, T. P.; Fitzpatrick, A. W.; Meehan, S.; Mott, H. R.; Vendruscolo, M.; Dobson, C. M.; Welland, M. E. *Science*, **2007**, *318*,1900–1903.

(3) Hall, C. K.; Wagoner, V. A. *Methods Enzymol.*, **2006**, *412*, 338–365.

(4) Ma, B. Y.; Nussinov, R. *Curr. Opin. Chem. Biol.*, **2006,** *10*, 445–452.

(5) Tsai, C. J.; Zheng, J.; Nussinov, R. *PLoS Comput. Biol.*, **2006**, *2*, 311-319.

(6) Mahler, A.; Reches, M.; Rechter, M.; Cohen, S.; Gazit, E. *Adv. Mater.*, **2006**, *18*, 1365-1370.

(7) Reches, M.; Gazit, E. *Science*, **2003**, *300*, 625-627.

(8) Görbitz, C. H. *Chem. Commun.*, **2006,** *14*, 2332-2334;

Henrik, C.; Görbitz, C. H. *Chem. Eur. J.*, **2007**, *13*, 1022-1031.

(9) Görbitz, C. H. *Chem. Eur. J.*, **2001**, *7*, 5153-5159.

(10) Song, Y. J.; Challa, S. R.; Medforth, C. J.; Qiu, Y.; Watt, R. K.; Pena, D.; Miller, J. E.; van Swol, F.; Shelnutt, J. A. *Chem. Commun.*, **2004**, *7*, 1044-1045.

(11) Reches, M.; Gazit, E. *Nano Letters*, **2004**, *4*, 581-585.

(12) Gazit, E. *FASEB J*. **2002**, *16*, 77-83.

(13) Azriel, R.; Gazit, E. *J. Biol. Chem.*, **2001**, *276*, 34156-34161.

(14) Huang, R.; Qi, W.;Su, R.; Zhao, J.; He, Z. *Soft Matter*, **2011**, *7*, 6418-6421.

(15) Charalambidis, G.; Kasotakis, E.; Lazarides, Th.; Mitraki, A.; Coutsolelos, A. G. *Chemistry Eur. J.*, **2011**, *17*, 7213-7219.

(16) Smith, A. M.; Williams, R. J.; Tang, C.; Coppo, P.; Collins, R. F.; Turner, M. L.; Saiani, A.; Ulijn, R. V. *Advanced Materials*, **2008**, *20*, 37-41.

(17) Orbach, R.; Adler-Abramovich, L.; Zigerson, S.; Mironi-Harpaz, I.; Seliktar, D.; Gazit, E. *Biomacromolecules*, **2009**, *10*, 2646-2651.

(18) Orbach, R.; Mironi-Harpaz, I.; Adler-Abramovich, L.; Mossou, E.; Mitchell, E. P.; Forsyth, V. T.; Gazit, E.; Seliktar, D. *Langmuir*, **2012**, *28*, 2015-2022.

(19) Uversky, V. N.; Narizhneva, N. V.; Kirschstein, S. O.; Winter, S.; Lober, G. *Fold. Des.* **1997**, *2*, 163-172.

(20) Buck, M. Q. *Rev Biophys.* **1998**, *31*, 297-355.

(21) Hwang, S.; Shao, Q.; Williams, H.; Hilty, C.; Gao, Y. Q. *J. Phys. Chem. B*, **2011**, *115,* 6653-6660.

(22) Tamamis, P.; Adler-Abramovich, L.; Reches, M.; Marshall, K.; Sikorski, P.; Serpell, L.; Gazit, E.; Archontis, G. *Biophys. J.*, **2009**, *96*, 5020-5029.

(23) Villa, A.; van der Vegt, N. F. A.; Peter, C. *Phys. Chem. Chem Phys*., **2009**, *11*, 2068-2076; Villa, A.; Peter, C.; van der Vegt, N. F. A. *Phys. Chem. Chem. Phys*., **2009**, *11*, 2077-2086.

(24) Frederix, P. W. J. M; Ulijn, R. V.; Hunt, N. T.; Tuttle, T. *J. Phys. Chem. Lett*., **2011**, *2(19)*, 2380-2384.

(25) Guo, C.; Luo, Y.; Zhou, R.; Wie, G. *ACS Nano*, **2012**, *6*, 3907-3918.

(26) Renzi, D.; Carlevaro, C. M.; Stoico, C.; Vericat, F. *Molecular Phys.*, **2001,** *99*, 913-922.

(27) Berendsen, H.; van der Spoel, D.; van Drunen, R. *Comp. Phys. Comm*., **1995**, *91*, 43-56.

(28) Lindahl, E.; Hess, B.; van der Spoel, D. *J. Mol. Model.*, **2001**, *7*, 306-317.

(29) Hess, B.; Kutzner, C.; van der Spoel, D.; Lindahl, E. *Journal of Chemical Theory and Computation*, **2008**, *4*, 435-447.

(30) Bussi, G.; Donadio, D.; Parinello, M. *J. Chem. Phys.*, **2007**, *126*, 014101_1 – 014101_7.

(31) Oostenbrink, C.; Villa, A.; Mark, A. E.; van Gunsteren, W. F. *J. Comput. Chem.*, **2004**, *25*, 1656-1676.

(32) Berendsen, H. J. C.; Postma, J. P. M.; van Gunsteren, W. F.; Hermans, J. *Pullman, B. ed. D. Reidel Publishing Company Dordrecht*, **1981**, 331-342.

(33). Swendsen, R; Wang, J. *Phys. Rev. Lett.*, **1986**, *57*, 2607–2609.

(34) Hansmann, U. H. E. *Chem. Phys. Lett.*, **1997**, *281*, 140–150.

(35) Sugita, Y.; Okamoto, Y. *Chem. Phys. Lett.*, **1999**, *314*, 141–151.

(36) Nymeyer, H.; Gnanakaran, S.; Garcia, A. E. *Methods Enzymol.*, **2004**, *383*, 119–149.

(37) Hukushima, K.; Nemoto, K. *J. Phys. Soc. Jpn.*, **1996**, *65*, 1604–1608.

(38) Sanbonmatsu, K. Y.; Garcia, A. E. *Proteins*, **2002**, *46***,** 225–234.

(39) Kumar, R.; Schmidt, J. R.; Skinner, J. L. *J. Chem. Phys*., **2007**, *126*, 204107-204119.

(40) Haughney, M.; Ferrario, M.; McDonald, I. R. *Mol. Phys*., **1986**, *58*, 849-853.

(41) Haughney, M.; Ferrario, M.; McDonald, I. R. *J. Phys. Chem*., **1987**, *91*, 4934-4940.

(42) Kim, J.; Han, T. H.; Kim, Y.; Park, J. S.; Choi, J.; Churchill D. G.; Kim, S. O.; Ihee, H. *Adv. Mater*., **2010**, *22*, 583-587.

(43) Tamamis, P.; Kasotakis, E.; Mitraki, A.; Archontis, G. *J. Chem. Phys. B*, **2009**, *113*, 15639-15647.

(44) Harmandaris, V.; Kremer, K. *Soft Matter*, **2009**, *5*, 3920-3926; *Macromolecules*, **2009**, *42*, 791-802.